Effects of additional multiwall carbon nanotubes on impact behaviors of $LiNi_{0.5}Mn_{0.3}Co_{0.2}O_2$ battery electrodes

Anh V. Le,[1] Meng Wang,[1] Yang Shi,[2] Daniel Noelle,[2] Yu Qiao,[1,2] and Weiyi Lu[3,a)]
[1]*Department of Structural Engineering, University of California San Diego, La Jolla, California 92093-0085, USA*
[2]*Program of Materials Science and Engineering, University of California San Diego, La Jolla, California 92093, USA*
[3]*Department of Civil and Environmental Engineering, Michigan State University, East Lansing, Michigan 48824, USA*

(Received 12 May 2015; accepted 16 August 2015; published online 28 August 2015)

This work introduces a new mechanically triggered thermal runaway mitigation mechanism. The homogenizer of electrode failure (HEF), multiwall carbon nanotube (MWCNT), was added into $LiNi_{0.5}Mn_{0.3}Co_{0.2}O_2$ (NMC532) battery electrodes. We have studied the effect of the HEF additive on the internal electrical resistance and the mechanical impact resistance of the electrodes. The additional MWCNTs reduced the internal electrical resistance of electrodes before mechanical abuse. Upon mechanical abuse, they could mitigate internal shorting and thermal runaway at normal battery working temperature. © *2015 AIP Publishing LLC*.
[http://dx.doi.org/10.1063/1.4929647]

I. INTRODUCTION

To reduce greenhouse gas emission and to enhance energy security, it is desirable that next-generation vehicles can be electrically powered.[1] With the success of hybrid vehicles and electric control components,[2] currently, the "bottleneck" of electric vehicle (EV) development is the energy storage system.[3]

In order to reach a drive range of 310 miles, the average value of all combustion vehicles about 86 kWh energy must be stored;[4] and to minimize the battery weight, high energy density lithium (Li) ion batteries are preferred.[5] At the cell level, the energy density is around 100–200 Wh/kg. Thus, to provide sufficient energy, nearly 400 kg of battery cells have to be carried, and the total battery system, including module and pack components as well as battery thermal management system (BTMS), can be heavier than half a ton. Higher energy Li-ion batteries and/or more efficient battery system design must be developed to reduce the system weight, for which intensive studies are being conducted.[6–8]

The safety of Li-ion batteries imposes another tough challenge. While battery management systems (BMS) and BTMS can ensure safe operation of batteries under working condition, upon mechanical abuse, e.g., in a traffic accident, battery components could be broken apart. A Li-ion battery consists of a cathode and an anode, and a porous polymer membrane separator in between them.[9] To minimize internal impedance, the membrane separator must be quite thin, usually ~10 μm thick. When the membrane ruptures, the active materials in cathode and anode would directly contact with each other, leading to internal shorting. As temperature increases, the electrochemical reactions speed up,[10] which worsens the situation and eventually, causes thermal runaway; that is, the battery system loses its stability and in a few minutes the temperature would rise to beyond the safety range.[11] The electrolyte in a regular Li-ion battery is often based on ethyl methyl carbonate (EMC) or dimethyl carbonate (DMC). When temperature reaches 90–120 °C, the metastable solid-electrolyte interface (SEI) layer starts to decompose, which is an exothermic reaction.[12] Even worse, when the boiling point of the solvent, 90 °C for DMC and 107 °C for EMC, is approached, concentration of the solvent vapor increases dramatically and the solvent-vapor mixture becomes highly flammable. The combustion heat of EMC or DMC is quite high, around 15 MJ/kg.[13] Assume the electrolyte mass is ~15% of the battery cell mass,[14] combustion of the batteries in an EV would generate a large amount of heat ~J, equivalent to that of nearly 25 l of gasoline.

In the past a couple decades, scholars investigated a few approaches to mitigate thermal runaway. Positive temperature coefficient (PTC) materials have been added in electrodes.[15] These additives do not affect normal battery operation; yet when temperature rises to a set point, they would increase the internal impedance, and thus, suppress further temperature increase. A special phase transition material (PTM) is low-melting-point membrane separator,[16] which melts and closes its pores as the melting point is exceeded. As the ion transportation path is shut down between the cathode and the anode, there is no return path to form a complete internal shorting circuit, and heat generation should stop after the "residual" charges carried by the entrapped electrolyte are consumed. However, the triggered thermal runaway mitigation mechanism (TRMM) takes time to be fully effective. Hence, there would be a considerable temperature "overshooting" in battery cell, even after TRMM begins to function.

In the current research, we investigate a mechanically triggered TRMM, by using homogenizers of electrode failure (HEF): As depicted in Figure 1, HEF can be mixed with the active materials (AMs) in an electrode as microparticulates.

a)Author to whom correspondence should be addressed. Electronic mail: wylu@egr.msu.edu.

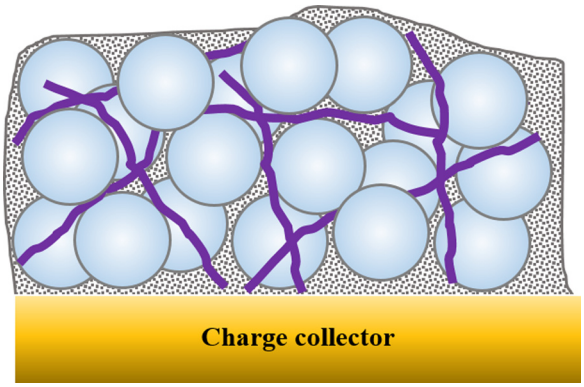

FIG. 1. Schematic of modified battery electrodes.

They are electrochemically neutral, having little influence on battery power and cycle life. Upon an external impact, HEF microparticulates debond from the electrode matrix, promoting widespread damages. With the homogenized failure, the internal impedance of electrode would largely increase, having a somewhat similar effect as the melting of separation membrane. Thus, the return path of internal shoring circuit is reduced and thermal runaway would be suppressed.

Electrochemical neutral materials include many polymers such as polypropylene (PP), polystyrene (PS), and polyethylene (PE); metals such as copper (Cu) and aluminum (Al); carbon materials (C); and ceramics such as silica. Membrane separators are often made of PP, PS, and/or PE; Cu and Al are used to produce charge collectors. Among these candidates, our study will be focused on carbon materials, particularly carbon nanotubes (CNT), as they are lightweight and of relatively stiff. A low mass density helps minimize reduction in battery power density; a high stiffness is energetically favorable to store elastic energy and trigger debonding and homogeneous cracking or voiding.[17] The high electrical conductivity of CNT makes it the best additive in cathode among carbon materials.[18] It can effectively reduce the internal electrical impedance,[18] reach high rate capability,[19,20] and increase energy capacity retention ratio.[21,22]

II. EXPERIMENTAL

In the current study, reference positive and negative electrode films and multiwall carbon nanotubes (MWCNTs) (SKU-030102, Cheaptube.com) modified ones were prepared. Outer diameter, inner diameter, length, and purity of the received MWCNTs were 8–15 nm, 3–5 nm, 10–50 μm, and >95 wt. %, respectively. For all electrode films, the polymeric binder used was polyvinylidene fluoride (PVDF) with molecular weight, M_w of 534k by G.P.C (182702, Sigma-Aldrich), and the conductive additive was carbon black (CB) (CNERGY C65, Timcal, Ltd.). For cathode, the AM is $LiNi_{0.5}Mn_{0.3}Co_{0.2}O_2$ (NMC532) (NCM-04ST, TODA America, Inc.), and the weight ratio of solid components is AM:PVDF:CB = 93:4:3. For anode, the active material was artificial graphite powder (EQ-Lib-CMSG, MTI Corp.), and the weight ratio among solid components is AM:PVDF:CB = 93:6:1. For modified cathode and anode films, the MWCNTs were added at an additional 1 wt. %, 3 wt. %, or 5 wt. % of the total solid components in the reference slurry (i.e., AM, PVDF, and CB).

The slurry processing was started with dissolving PVDF in 1-methyl-2-pyrrolidinone (NMP) (328634, Sigma-Aldrich). The amount of NMP solvent was 1:1 w/w with respect to the total mass of the solid components (i.e., AM, PVDF, and CB). Mechanical stirring was carried out at 500 rpm for 30 min by a PCVS1 mechanical stirrer (IKA, Inc.). After that, CB was added into the mixture to create a conductive network, and the solution was kept stirring at 500 rpm for another 30 min. When the CB was uniformly dispersed in the solution, AM was poured into the solution. The mixture was homogenized at 1500 rpm for 12 h until a uniformly dispersed slurry was achieved. For the MWCNTs modified film, after 30 min stirring of the reference slurry, a desired amount of MWCNTs was added into the slurry before homogenizing.

When the homogenization was complete, the slurry was cast onto the charge collector using the doctor blade method. Anode slurry was cast at 250 μm thickness on a 12 μm thick copper foil, and cathode slurry is cast at 600 μm thickness on an 18 μm thick aluminum foil. The wet slurries were dried under vacuum at 80 °C by a VWR 1410 vacuum oven for 24 h. Cathode sample modified by 5 wt. % activated carbon (Darco S-51, Norit Americas, Inc.) was prepared in the same procedure.

After drying, the NMP solvent was completely evaporated and the electrode films were firmly bonded to the charge collector. To optimize the porosity, the dried films were sandwiched by two flat stainless steel plates with smooth surfaces, compressed, and held at desired pressure for 30 s by an Instron 5582 Model. The compressive pressures were 15 MPa and 30 MPa for anode and cathode films, respectively. The compressed films were cut into 1 cm × 1 cm squares. All the sample films were crack free. Testing specimens, comprising 10-layers of these small films and saturated by 200 μl EMC, which is the solvent for Li-ion battery electrolyte, were used to represent the layered structure in real battery system.

An impact test on electrodes is performed using a laboratory-made table-top drop tower consisting of a solid stainless steel base, a solid metal holder and a transparent polycarbonate (PC) guide. The force applied on the samples was measured by an accelerometer (ACC103, Omega, Inc.) attached to the drop weight and recorded by a high speed digitizer (PCI-5105, National Instruments, Corp.). Due to difference in mechanical properties between cathode and anode films, two separate impact systems with similar set-up but different parameters were developed for dynamic testing. The specifications of the impact systems are listed in Table I, and the schematic of the experimental set-ups are shown in Figure 2.

TABLE I. Specification of the tabletop drop tower system.

Electrode	Material	Drop weight (kg)	Diameter (mm)	Length (mm)	Drop height (mm)
Cathode	Titanium	0.405	22.27	266	0–160 (~80)
Anode	Stainless steel	7.7	620	3050	4–22 (~12)

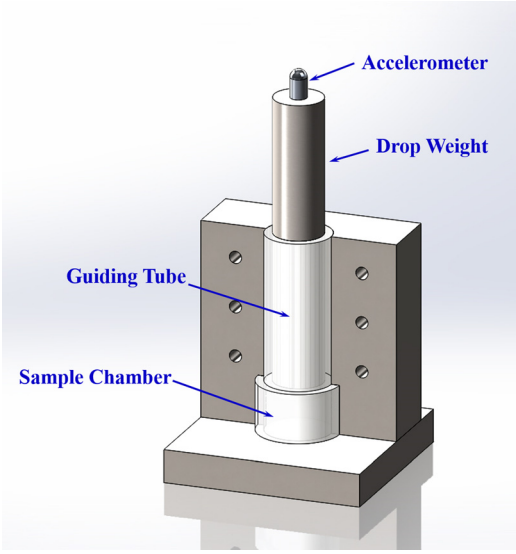

FIG. 2. Schematic of impact system.

III. RESULTS AND DISCUSSION

Electrical resistance was measured across 2 mm at the center of each electrode layer under different conditions: oven-dried (R_d), dried and compressed before impact (R_c), soaked in EMC before impact (R_s), and still wet condition after impact (R_i). The measurements for anode films are presented in Table II. By adding 3 wt. % of MWCNTs, the modified anode had much lower R_c than reference anode will lead to a much reduced energy consumption in the battery cell. The cathode films were more fragile than the anode ones. To avoid introducing surface cracks by the probes in resistance measurement, only the resistance of oven dried specimens was measured. The resistance was 241.3 ± 8.9, 156.5 ± 7.5, and 73.4 ± 6.5 Ω for cathodes containing 0 wt. %, 1 wt. %, and 5 wt. % MWCNTs, respectively. The 30% to 70% reduction of internal electrical impedance of the cathode films with increased amount of MWCNTs must be attributed to the excellent electrical conductivity of CNTs. In comparison, the additional 5 wt. % S-51 activated carbon reduced the resistance to 120.8 ± 6.7 Ω. Therefore, adding MWCNTs into both cathode and anode enhances the electrochemical performance of the Li-ion battery.

TABLE II. Resistance of a single layer of anode film under different conditions.

Sample	R_d (Ω)	R_c (Ω)	R_s (Ω)	R_i (Ω)
Reference anode	4.5–9	10–40	7–15.5	1–20
3 wt. % MWCNT anode	4–6.5	7.5–21	7–14	7–11

It had been expected that the damaged electrode after impact would exhibit a higher resistance compared to intact ones before impact. Due to the large deviation of measured data, this theory was not well supported by the experimental results. Another resistance measurement error might come from the different amount of evaporated electrolyte solvent. Hence, the resistance of electrolyte solution, part of the total electrode resistance,[22] was not a constant in each individual sample. However, the microscopic pictures of the electrode films in Figure 3 did show that the MWCNT additive was indeed effective in crack generation for both cathode and anode materials. The reference samples of both cathode and anode had good impact resistance and no crack was generated after impact. As shown in Figure 3(a), when cathode film was modified by 1 wt. % MWCNTs, only one surface crack was observed in one layer of the stack indicating that there is a critical loading fraction of HEF microparticulates below which no widespread damages would be introduced in the electrode film. When the content of MWCNT was increased to 5% and 3% in cathode and anode films, respectively, pronounced cracks at the center of all electrode films were observed. Similar trend was observed in S-51 activated carbon modified electrodes. However, the crack density was much lower than MWCNT modified electrodes. With increased amount of MWCNTs in unit area, although the elastic energy stored in each MWCNT was less, the resistance to crack initiation was also decreased as the spacing between MWCNTs was smaller. In addition, the MWCNTs were much stiffer than the surrounding electrode materials. Apparently, there is an upper limit of the loading fraction of MWCNTs at which the elastic energy stored in each MWCNT is too low to overcome the bonding strength between the electrode material and

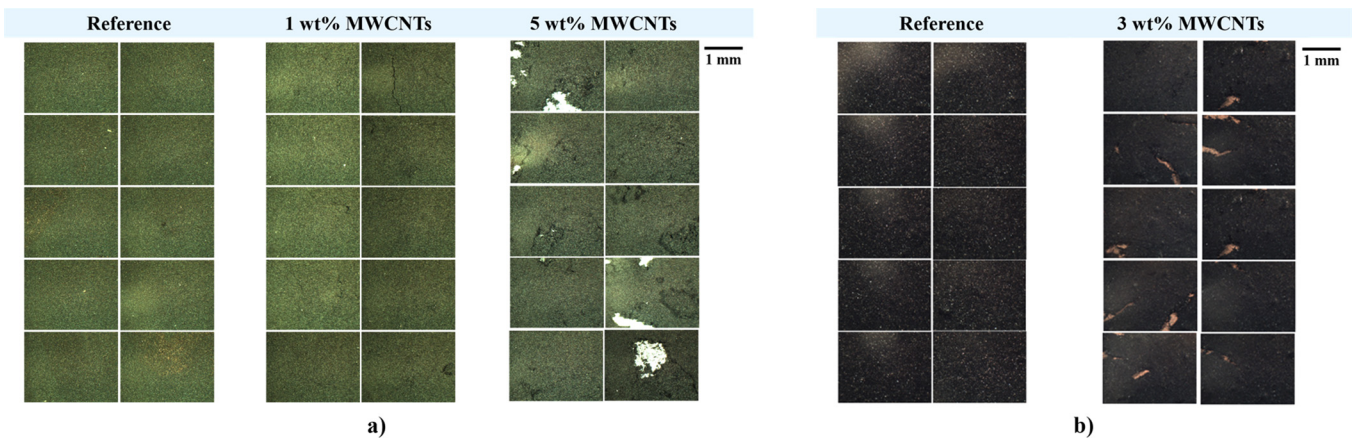

FIG. 3. Optical microscopic photos of electrode film stacks after drop tower tests (a) cathode samples with 0 wt. %, 1 wt. %, and 5 wt. % load of MWCNTs and (b) anode samples with 0 wt. % and 3 wt. % load of MWCNTs.

the substrate. The crack initiation and propagation can be optimized by selecting loading fraction of MWCNTs in between the lower and upper limits.

From the deceleration profile of the drop weight/impactor, the stress history applied on the electrode stack was calculated and presented in Figure 4. The stress rising rate of reference samples, i.e., the slope of curves "AB" and "CD" in Figures 4(a) and 4(b), was much higher than those of MWCNT modified electrodes. Since 1 wt. % of MWCNTs was below the critical value, the stack had similar dynamic response as the reference and its loading history can be treated as reference profile for cathode. The Young's modulus of samples can be expressed as

$$E = \Delta\sigma/(\Delta x/d_0), \tag{1}$$

where σ is the stress applied on the specimen, x is the displacement, and d_0 is the original thickness of the stack. The displacement can be calculated as

$$x = \int_{t_1}^{t_2} \left\{ \sqrt{2gh} - \int_{\tau_1}^{\tau_2} [\sigma(s)A/m]ds \right\} d\tau, \tag{2}$$

where g is the acceleration of gravity, h is the drop height, A is the cross-sectional area of the electrode specimen, and m is the mass of the impactor. The anode film with a Young's modulus of 507 MPa is much stiffer than the cathode one with a value of 53.6 MPa.

In general, CNT reinforced composites possess increased stiffness and yield strength, since the loading fraction and the surface condition of CNT were optimized. However, as shown in Figure 4, the smaller stress gradient, 33.5 MPa for anode with 3 wt. % MWCNTs and 15.2 MPa for cathode with 5 wt. % MWCNTs, indicating that the additional MWCNTs effectively reduced overall stiffness of modified samples. This is mainly because wide spread cracks after impact were desired rather than reinforcement. It is also due to the random orientation of MWCNTs in the electrode films. The stiffness of MWCNTs along the axis direction is extremely high while in directions perpendicular to the tube axis the value is low. In addition, the MWCNTs were not straight and the effective stiffness of the structure might be even lower.

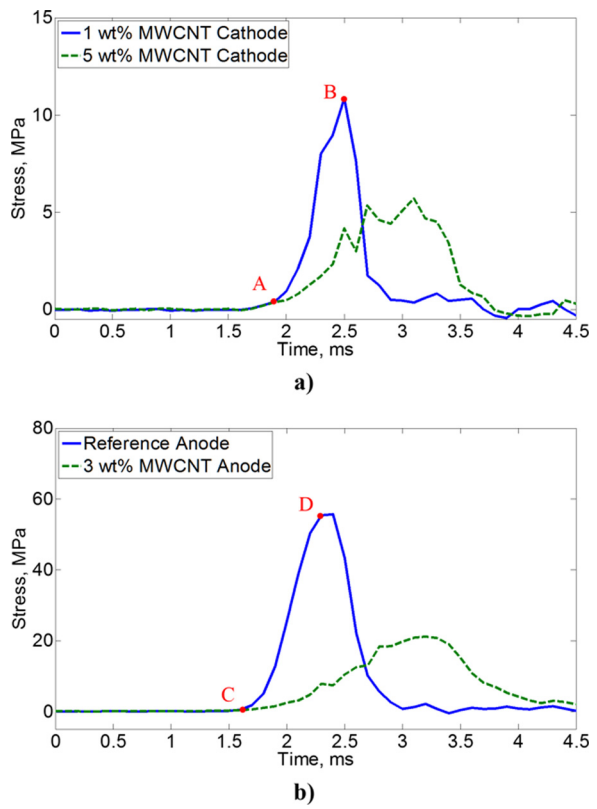

FIG. 4. Stress histories on electrode film stacks (a) cathode samples and (b) anode samples.

The energy associated with the references and modified samples in each test can be calculated by in the following equation and the values are listed in Table III:

$$U = \int \sigma A dx. \tag{3}$$

They were close to the input kinetic energy of the impactor, in both cathode and anode cases. However, in reference specimens, the energy was temporarily stored as elastic energy and no permanent damages were developed because the stress rising rate was linear until the peak stress was reached. The modified samples underwent plastic deformation as indicated by the sharp turning points of the stress profiles in Figure 4. About 90% of the kinetic energy was dissipated by both modified cathode and anode films. The amount of absorbed energy was directly related to the load fraction of MWCNTs, since it was the additional surface energy of the new cracks promoted by the MWCNT debonding. The surface energy was proportional to the elastic energy release rate, G_c, a material constant and the density of cracks as described in the following equation:

$$E_s = 2G_c A_c, \tag{4}$$

where $2A_c$ is the total new surface area associated with the cracks.

The fracture strength of modified samples was also determined by the amount of MWCNTs. The values for reference samples were higher than the applied stress range (11 MPa for cathode reference and 60 MPa for anode reference), since the samples were still in the elastic range. The fracture strength of modified films can be directly read off from Figure 4, which were 4.2 MPa and 7.8 MPa for modified cathode and anode film stacks, respectively. It is defined as the stress level of the first sharp turning point on the stress profile. When the applied stress is lower than fracture

TABLE III. Kinetic energy of drop weight and energy associated with all electrode samples.

Sample	Kinetic energy of impactor (J)	Elastic energy stored in reference samples (J)	Plastic energy dissipated in modified samples (J)
Cathode	0.32	0.40	0.32
Anode	0.90	0.90	0.82

strength, the local stress intensity is smaller than the fracture toughness and the electrodes are in normal working condition. Once the external stress level is over the safety threshold, the elastic energy stored in stiffer MWCNTs is released which breaks their bonds with the polymeric binder. Consequently, large number of cracks can be introduced into the electrodes and cut-off the electrochemical reaction in the battery when the working temperature is still in the normal range.

IV. CONCLUSION

In conclusion, by adding small amount of MWCNTs into NMC 532 Li-ion battery electrodes, at normal working condition, the internal electrical resistance can be significantly reduced, and thus, improve the electrochemical behavior of the batteries. On the other hand, when mechanical abuse takes place and exceeds safety range, HEF microparticulates such as MWCNTs can be mechanically triggered and promote large density of cracks in both electrodes. Hence, both internal shorting and thermal run away can be suppressed at normal working temperature of Li ion batteries. In addition, the modified battery electrodes have large energy absorption capacity.

ACKNOWLEDGMENTS

This research was supported by the Advanced Research Projects Agency-Energy (ARPA-E) under Grant No. DE-AR0000396, for which we are grateful to Dr. Ping Liu and Dr. John Lemmon.

[1]S. Pacala and R. Socolow, Science **305**, 968 (2004).
[2]K. C. Bayindir, M. A. Gozukucuk, and A. Teke, Energy Convers. Manage. **52**, 1305 (2011).
[3]A. Khaligh and Z. H. Li, IEEE Trans. Veh. Technol. **59**, 2806 (2010).
[4]G. J. Offer, D. Howey, M. Contestabile, R. Clague, and N. P. Brandon, Energy Policy **38**, 24 (2010).
[5]M. Broussely, J. P. Planchat, G. Rigobert, D. Virey, and G. Sarre, J. Power Sources **68**, 8 (1997).
[6]G. Girishkumar, B. McCloskey, A. C. Luntz, S. Swanson, and W. Wilcke, J. Phys. Chem. Lett. **1**, 2193 (2010).
[7]X. Su, Q. L. Wu, J. C. Li, X. C. Xiao, A. Lott, W. Q. Lu, B. W. Sheldon, and J. Wu, Adv. Energy Mater. **4**, 1300882 (2014).
[8]G. Kucinskis, G. Bajars, and J. Kleperis, J. Power Sources **240**, 66 (2013).
[9]J. W. Wen, Y. Yu, and C. H. Chen, Mater. Express **2**, 197 (2012).
[10]Q. S. Wang, P. Ping, X. J. Zhao, G. Q. Chu, J. H. Sun, and C. H. Chen, J. Power Sources **208**, 210 (2012).
[11]D. Doughty and E. P. Roth, Electrochem. Soc. Interface **21**, 37 (2012).
[12]R. Spotnitz and J. Franklin, J. Power Sources **113**, 81 (2003).
[13]S. J. Harris, A. Timmons, and W. J. Pitz, J. Power Sources **193**, 855 (2009).
[14]L. Gaines and R. Cuence, Argonne National Laboratory Technical Report ANL/ESD-42 (2000).
[15]H. Zhong, C. Kong, H. Zhan, C. M. Zhan, and Y. H. Zhou, J. Power Sources **216**, 273 (2012).
[16]P. Arora and Z. M. Zhang, Chem Rev. **104**, 4419 (2004).
[17]A. Lekatou, S. E. Faidi, S. B. Lyon, and R. C. Newman, J. Mater. Res. **11**, 1293 (1996).
[18]G. P. Wang, Q. T. Zhang, Z. L. Yu, and M. Z. Qu, Solid State Ionics **179**, 263 (2008).
[19]X. L. Li, F. Y. Kang, X. D. Bai, and W. C. Shen, Electrochem. Commun. **9**, 663 (2007).
[20]A. Varzi, C. Taubert, M. Wohlfahrt-Mehrens, M. Kreis, and W. Shutz, J. Power Sources **196**, 3303 (2011).
[21]W. Wei, L. L. Guo, X. Y. Qiu, P. Qu, M. T. Xu, and L. Guo, RSC Adv. **5**, 37830 (2015).
[22]X. M. Liu, Z. D. Huang, S. W. Oh, B. Zhang, P. C. Ma, M. Yuen, and J. K. Kim, Compos. Sci. Technol. **72**, 121 (2012).